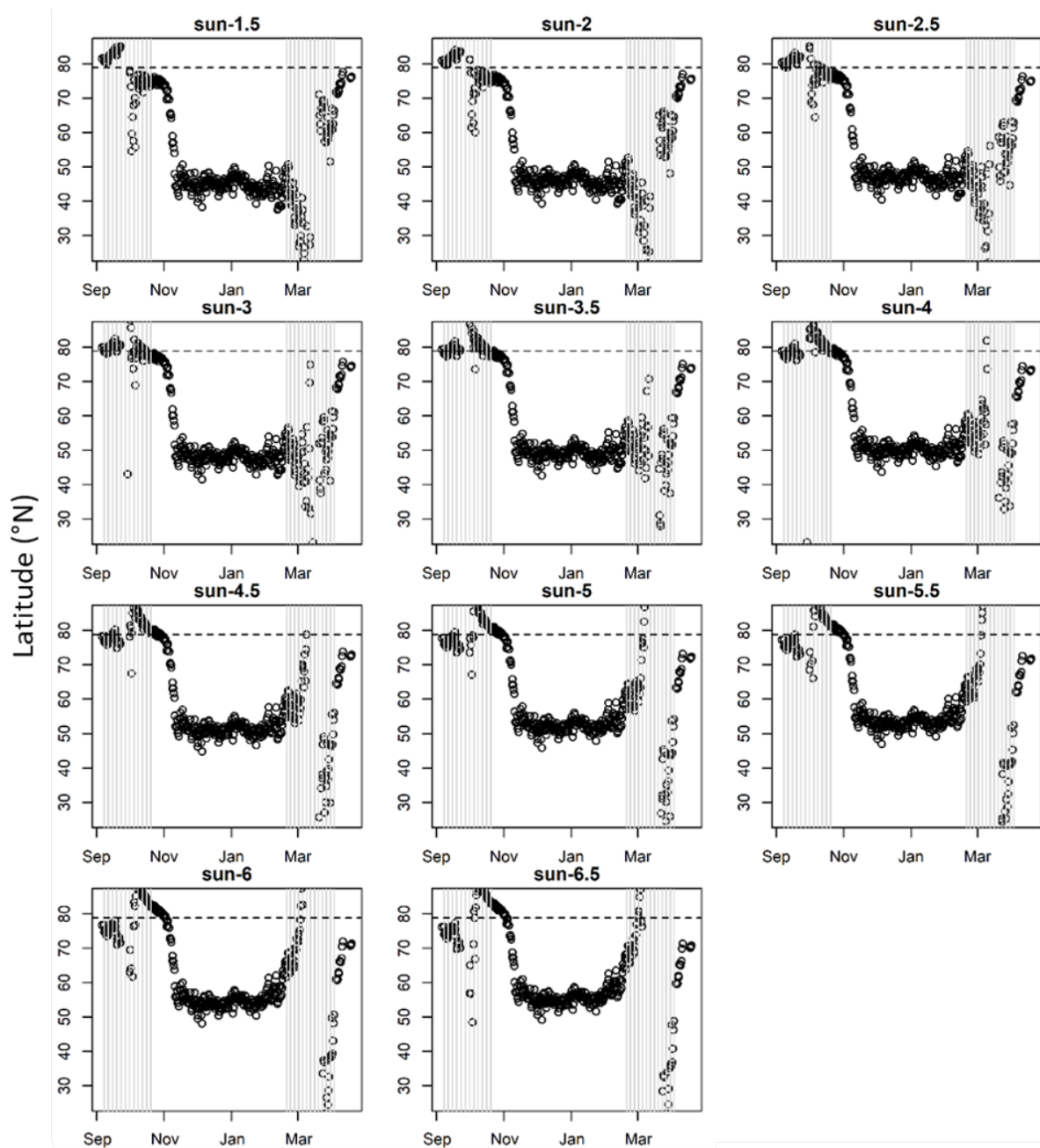
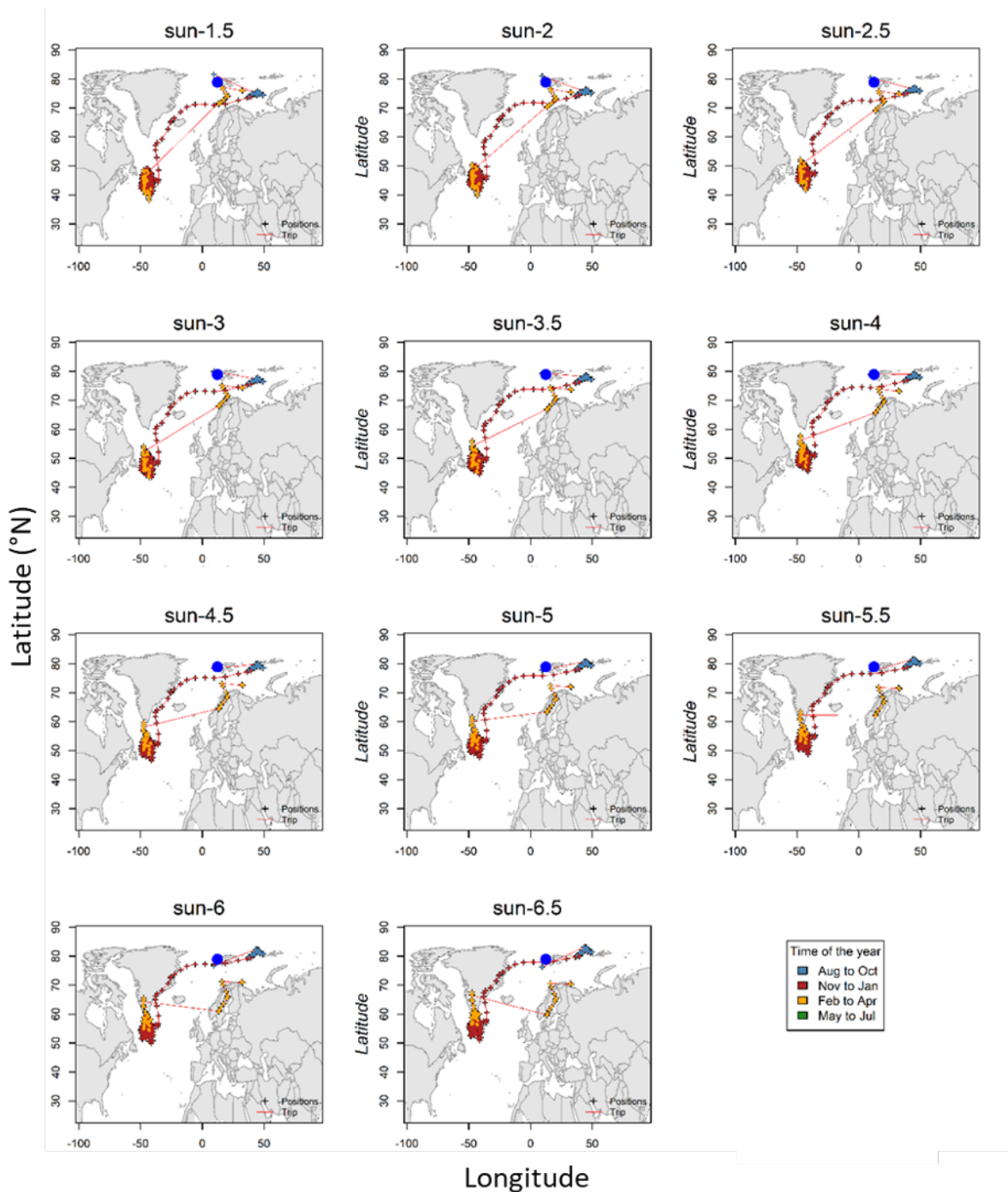


## SUPPLEMENT



**Figure S1.** Example of sun elevation angle selection from Bråthen et al. (2021) for a black-legged kittiwake track (individual #17507, from June 2011 to June 2012). For each annual track, latitude versus time is plotted for different sun elevation angles and the sun elevation angle selected (1) minimized the amplification of the latitudinal error close to the equinoxes, (2) resulted in matching latitudes at both sides of the equinox, and (3) resulted in positions that fitted the latitude of the colony (Kongsfjorden, Svalbard; 78°52' N) at the beginning and the end of the track. In this example, we selected  $-3.0^\circ$  as the appropriate sun elevation angle mainly from criteria (1) and (3), since the bird moved north during the spring equinox period, making criteria (2) less useful here. The horizontal dotted line shows the latitude of the colony, and the vertical grey lines indicate the periods around autumn and spring equinoxes.



**Figure S2.** Example of sun elevation angle selection using the methods described in Bråthen et al. (2021) for a black-legged kittiwake track (individual #17507, same track as in Figure S1). Smoothed and filtered positions were calculated with different sun elevation angles. In combination with the steps illustrated in Figure S1, these maps supported the selection of  $-3.0^\circ$  as sun elevation angle, as they resulted in a track that best fitted the shape and position of the oceans and continents. The location of the colony (Kongsfjorden, Svalbard;  $78^\circ$  N,  $12^\circ$  E) is marked with a filled blue circle, and positions are coloured by time of the year. Positions from the equinox periods have been excluded from the map.

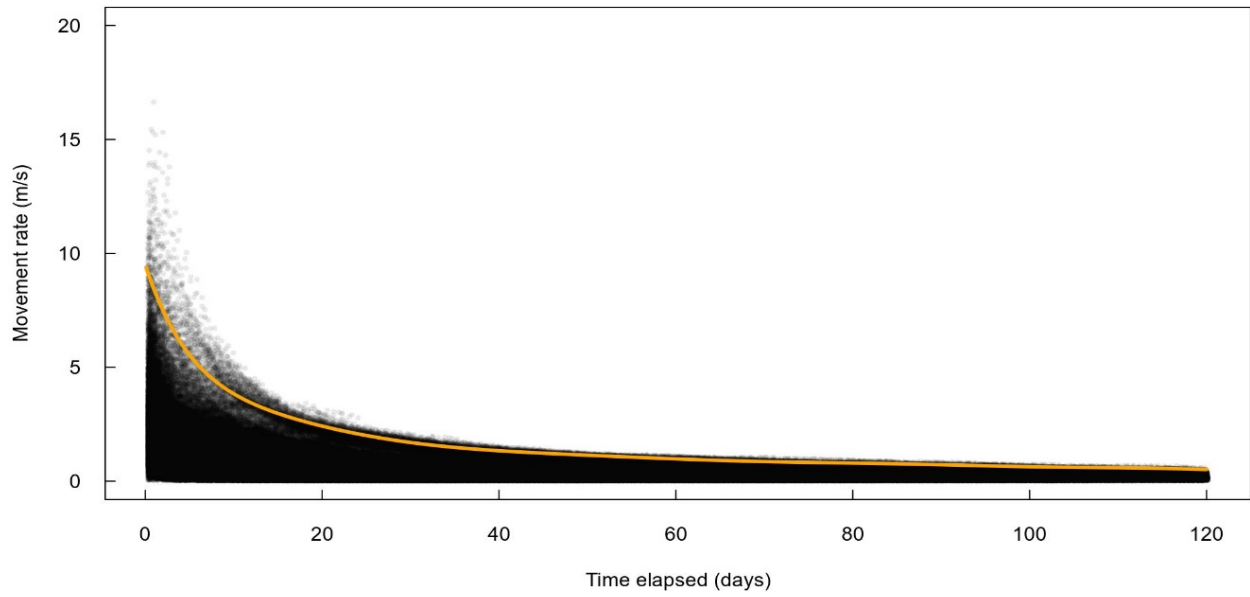


**Figure S3.** Movement rate plotted against time elapsed between two locations, for black-legged kittiwakes. The orange curve represents the 99<sup>th</sup> percentile predicted from a quantile regression model.

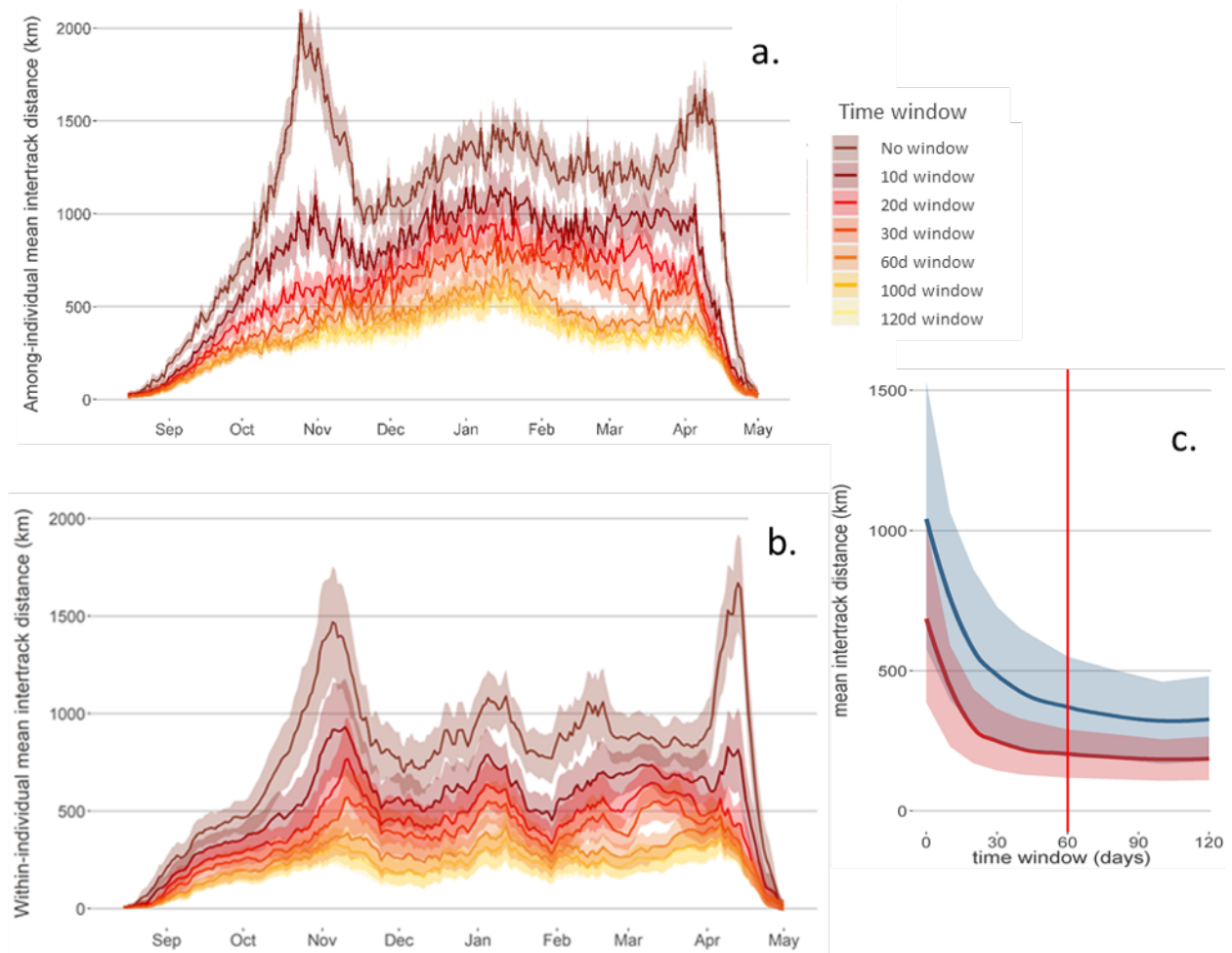


**Figure S4.** Comparison of variation among individuals (a. and blue line in c.) and within individual (b. and red line in c.) in mean intertrack distances estimated using different time windows. The increase in the time-window duration results in a gradual fading of timing effects, which are otherwise particularly strong during migration periods (Oct–Nov and Apr). The 60 d time window selected allows for comparison of tracks where dissimilarities mostly originate from spatial differences.

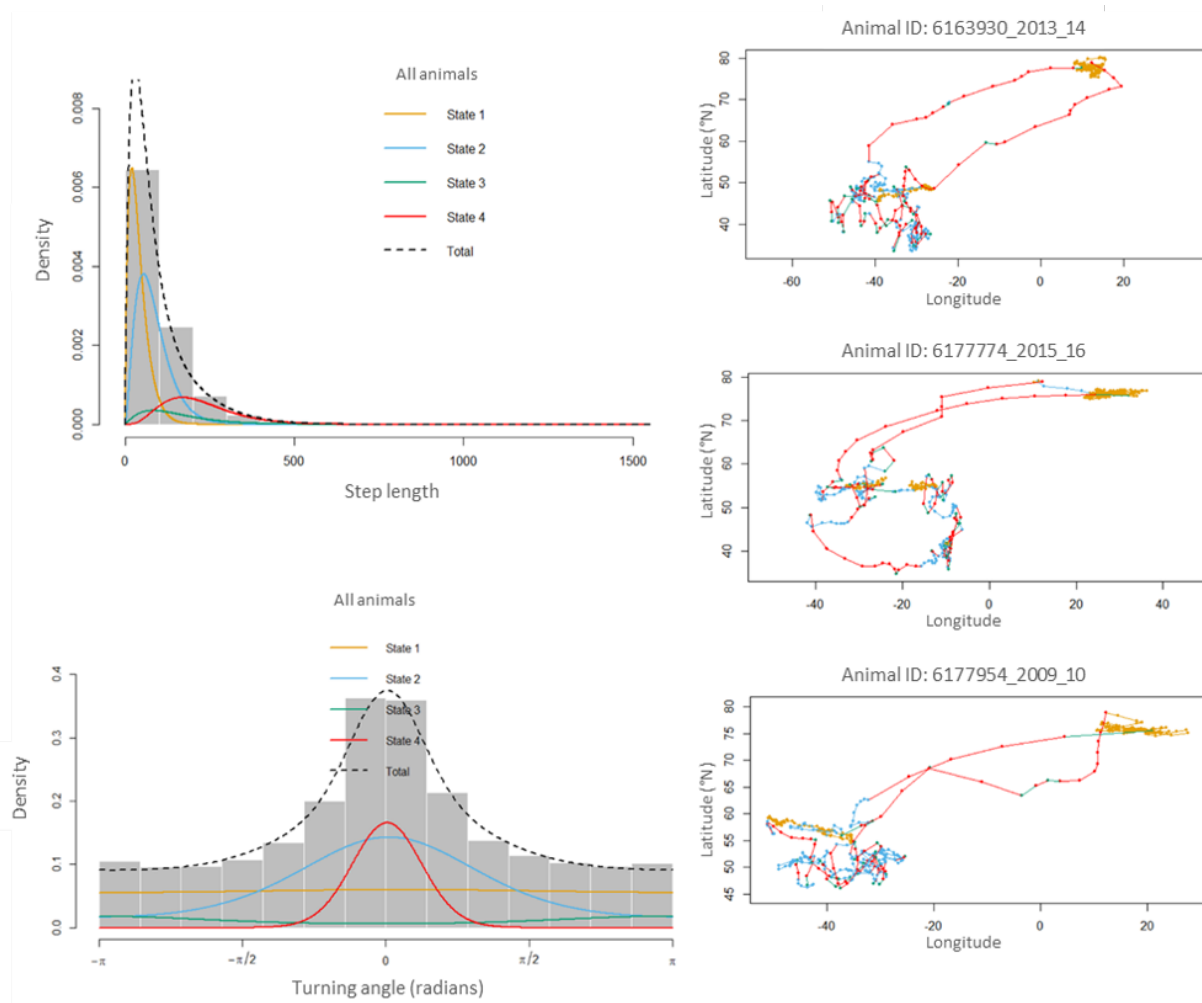


**Figure S5.** Distribution of step length (top left panel) and turning angle (bottom left panel) used in the final four-state Hidden Markov model selected to identify the sequence of behavioural states along the non-breeding tracks of individuals, with three tracks as examples. The States 1 (orange) and 2 (blue) were defined by short steps (<85 km on average) with either frequent shifts in direction (State 1) or moderately directional movement (State 2) and attributed to periods of staging in more intensively utilized areas, while the States 3 (green) and 4 (red) were defined by long steps (>150 km on average) with moderate shifts in direction (State 3) or highly directional movement (State 4) that characterized transient and commuting behaviours during travelling periods.

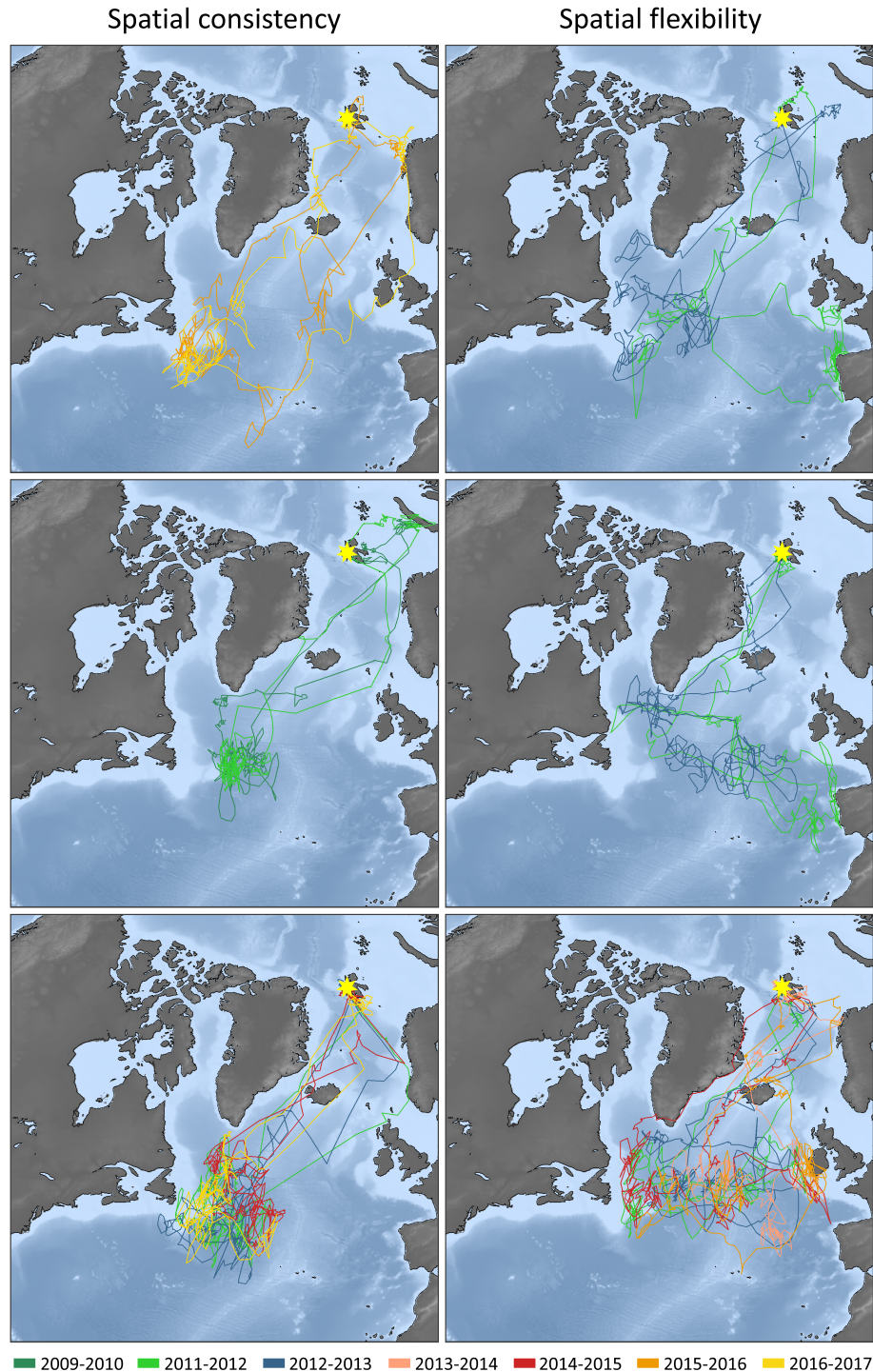


**Figure S6.** Examples of non-breeding tracks from six individuals tracked multiple years (from 2 to 5 years). The left panels show individuals displaying high interannual spatial consistency (mean nearest neighbour distance < 200 km) and the right panels show individuals displaying more flexibility in their non-breeding movement (mean nearest neighbour distance > 400 km), with shifting and itinerancy behaviours. Each colour represents one year of tracking (from the colony departure in fall to the colony arrival in spring). The yellow asterisk indicates the colony location.

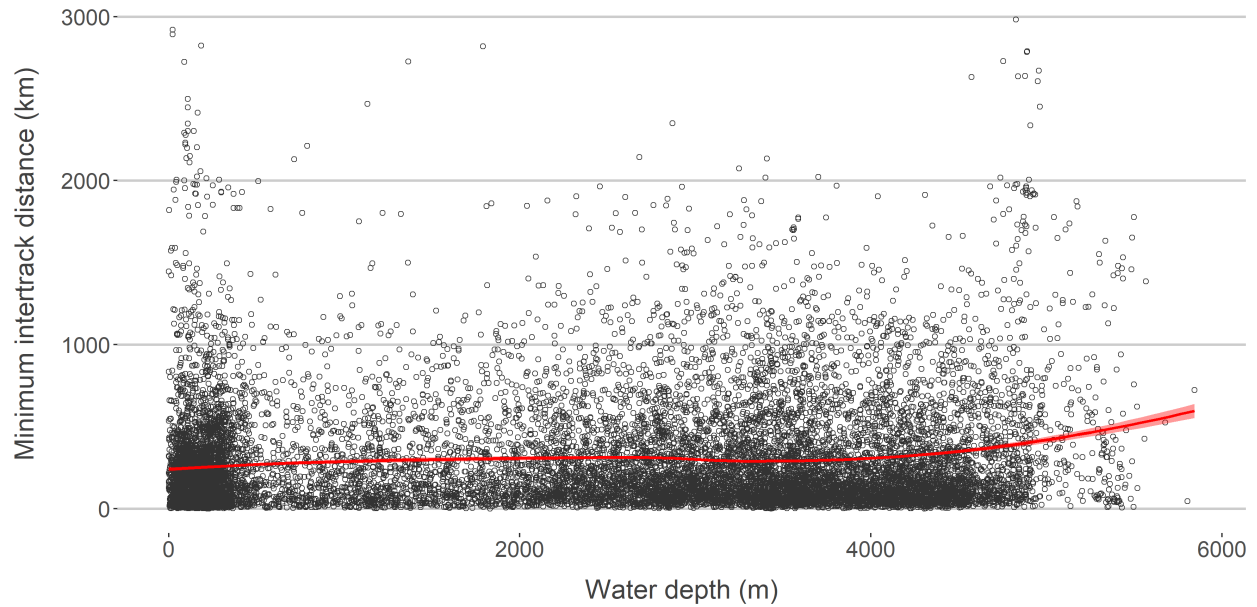


**Figure S7.** Within-individual spatial consistency over the ocean water depth. The red line is the moving average (using ‘loess’ smoother) of the intertrack minimum distances ( $\pm$ SE) and indicates that the individual site fidelity remains high over deep-water areas (depth > 500 m). The curve is plotted over the raw minimum intertrack distance data (black dots) estimated through the nearest neighbour distance analysis using a 60 d time window.

**Table S1.** Global location sensors (GLS) deployed and retrieved at the black-legged kittiwake colony in Kongsfjorden (Svalbard, Norway) between 2008 and 2019 and the number of complete annual tracks acquired and used in the analyses. The complete tracks were obtained after filtering for partial tracks caused by GLS failure or battery discharge. The GLS can be retrieved 2 or 3 yr after deployment and can record up to 2 complete annual tracks before battery discharge. NA: Not Applicable

Year	Number of GLS deployed	Number of GLS retrieved	Complete tracks recovered
2008	10	NA	NA
2009	11	8	8
2010	12	11	11
2011	56	12	2
2012	19	50	45
2013	20	13	15
2014	18	17	14
2015	25	13	13
2016	43	18	18
2017	21	39	21
2018	41	16	24
2019	NA	31	29
Total	276	228	200

**Table S2.** Mean (and SD) difference in number of days in the observed timing variation of phenological events estimated at the population level (i.e. variation among individuals) and at the intra-individual level (i.e. variation among years for individuals tracked multiple years).

Phenological parameter	Stage	Population level		Intra-individual level	
		Mean	SD	Mean	SD
Colony departure (no. of days)	Fall migration	18.4	9.5	12.5	9.8
Start of migratory movement (no. of days)	Fall migration	24.1	17.3	10.3	11.2
Crossing of the Arctic Circle (no. of days)	Fall migration	20.1	13.1	9.9	8.3
Start of migratory movement (no. of days)	Spring migration	8.4	9.4	6.1	3.7
Colony arrival (no. of days)	Spring migration	10.7	11.0	7.9	9.9



**Table S3.** Individual repeatability ( $r$ ) in timing of phenological events of fall and spring migrations of black-legged kittiwakes *Rissa tridactyla* breeding in Svalbard, where 0 corresponds to low repeatability and 1 to high repeatability. Also shown are associated standard error, confidence interval (CI), and p-value. Only individuals tracked multiple years were included (n = 104 repeated tracks from 33 individuals).

Phenological parameter	Stage	$r$	SE	CI	p
Colony departure <sup>a</sup>	Fall migration	0.203	0.096	0.020 – 0.390	<0.001
Start of migratory movement	Fall migration	0.796	0.058	0.653 – 0.880	<0.001
Crossing of the Arctic Circle	Fall migration	0.542	0.096	0.328 – 0.691	<0.001
Start of migratory movement	Spring migration	0.363	0.112	0.122 – 0.553	0.002
Colony arrival	Spring migration	0.277	0.115	0.038 – 0.494	0.016

<sup>a</sup>‘year’ included as a random factor to account for interannual variation in this parameter

**Table S4.** Frequency of step length and turning angle for each state used in four-state, three-state and two-state Hidden Markov Models. The final values of these parameters were defined after running iterations with varying initial values to ensure numerical maximization of the likelihood. We used *gamma* distribution to describe the step length frequency and *Von Mises* distribution to describe the turning angle frequency (i.e., angle concentration as a measure of the frequency of shifts in direction). The four-state model was selected after examination of the pseudo-residuals and because it better fitted the GLS data than the two- or three-state models based on Akaike’s Information Criterion (AIC) and initial inspection of distribution of movement parameters. NA: Not Applicable

Model	Parameter	State 1	State 2	State 3	State 4	AIC	
<b>Four-state</b>	Step length (km)	Mean ± SD	40.9 ± 29.3	84.5 ± 50.6	151.1 ± 102.6	218.9 ± 105.5	
	Turning angle	Mean	0.16	0.03	3.10	0.01	1244778
		Concentration	0.04	1.06	0.55	6.91	
<b>Three-state</b>	Step length (km)	Mean ± SD	42.7 ± 30.4	107.4 ± 71.3	215.8 ± 118.3	NA	
	Turning angle	Mean	0.04	0.04	0.01	NA	1252182
		Concentration	0.11	0.75	11.26	NA	
<b>Two-state</b>	Step length (km)	Mean ± SD	44.4 ± 31.5	139.4 ± 94.5	NA	NA	
	Turning angle	Mean	0.01	0.03	NA	NA	1261858
		Concentration	0.15	1.21	NA	NA	

## LITERATURE CITED

Bråthen VS, Moe B, Amélineau F, Ekker M and others (2021) An automated procedure (v2.0) to obtain positions from light-level geolocators in large-scale tracking of seabirds. A method description for the SEATRACK project. NINA Report 1893. Norwegian Institute for Nature Research. Trondheim, Norway. <https://hdl.handle.net/11250/2735757>